energy&fuels

pubs.acs.org/EF

Article

A Bottled High-Sulfur Fuel Oil Stranded with the Mysterious Oil Spill on the Brazilian Coast in Early 2022: Geochemical Correlation and Ocean Dumping Evidence

Published as part of Energy & Fuels special issue "Celebrating Authors of Energy and Fuels Most-Impactful Articles (2022)".

Rufino Neto A. Azevedo, Adriana P. Nascimento, Vinícius B. Pereira, Danielle M.M. Franco, Robert K. Nelson, Boniek Gontijo, Débora A. Azevedo, Ronaldo F. do Nascimento, Christopher M. Reddy,* Rivelino M. Cavalcante,* André H. B. Oliveira,* and Laercio L. Martins*

Cite This: *Energy Fuels* 2025, 39, 14254−14265

Read Online

ACCESS | Metrics & More | Article Recommendations | Supporting Information

ABSTRACT: This study conducted a comprehensive forensic geochemical and chemical assessment of bottled oil labeled with a foreign marine bunker company stranded on a Ceará beach, Northeast Brazil, in January 2022, and compared it to the mysterious oil spill that affected ∼342 km of the Ceará coast at that time. The saturated and aromatic composition was assessed by conventional gas chromatography (GC-FID and GC-MS) and comprehensive two-dimensional gas chromatography (GC × GC-FID). In addition, the bottled oil was also assessed by Fourier transform ion cyclotron resonance mass spectrometry (FT-ICR MS), CHNS elemental analyses, and microscopic imaging. The bimodal unresolved complex mixture (UCM) in the GC-FID chromatogram; the considerable abundance of anthracene, 2-methylanthracene, and other polycyclic aromatic hydrocarbons (PAHs) with four, five, and six rings; and the high abundance in carbon 40 observed for the N_1 class for the bottled oil are consistent with heavy fuel oil (HFO), probably an IFO 380. It has a high sulfur content (2.5%) outside the 2020 International Maritime Organization (IMO) specifications (%S < 0.5) unless the vessels are equipped with exhaust gas cleaning systems (EGCS or scrubbers). The fuel oil also has a high amount of catalytic fines, rich in Al and Si, which are known to damage marine engines and pose a potential threat to the environment. Resistant biomarkers (e.g., terpanes, steranes, C30 tetracyclic polyprenoids, and triaromatic steranes) and the GC-FID profile showed that this fuel oil geochemically correlates with the early 2022 oil spill, disclosing the spilled oil source from fuel dumping by an international tanker on the South Atlantic Ocean route. Fingerprint dissimilarities of the more volatile compounds indicate intense weathering or two different vessel fuel tanks. The high sulfur content and the presence of catalytic fines may explain the oil being disposed of into the sea.

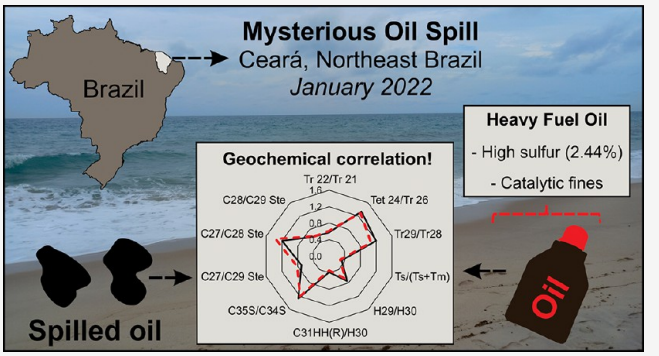

INTRODUCTION

Since the mysterious oil spill that contaminated ∼3200 km of the Brazilian shoreline in 2019, with ∼5000 tons of heavy oil dumped in the Atlantic Ocean,[1−5] the Brazilian scientific community has begun to constantly monitor the arrival of oil in the coastal region. Increased monitoring has revealed frequent orphan oil spills, particularly in northeastern Brazil, with distinct sources and proportions.[6−11] This constant contamination threatens the diverse marine ecosystem, vulnerable human communities, and essential economic activities such as fishing and tourism.[12−16] Furthermore, repeated oiling lengthens the recovery time of previously impacted areas. Understanding the timing, source, release location, impacted areas, and type of petroleum product is crucial for identifying trends that are useful in preparing for, responding to, and ideally preventing or limiting future costly incidents.

In January 2022, a new mysterious oiling occurred in Brazil, affecting the coast of Ceará. The spilled oil reached 84 beaches,

Received: March 25, 2025
Revised: June 27, 2025
Accepted: June 30, 2025
Published: July 14, 2025

https://doi.org/10.1021/acs.energyfuels.5c01581
Energy Fuels 2025, 39, 14254−14265

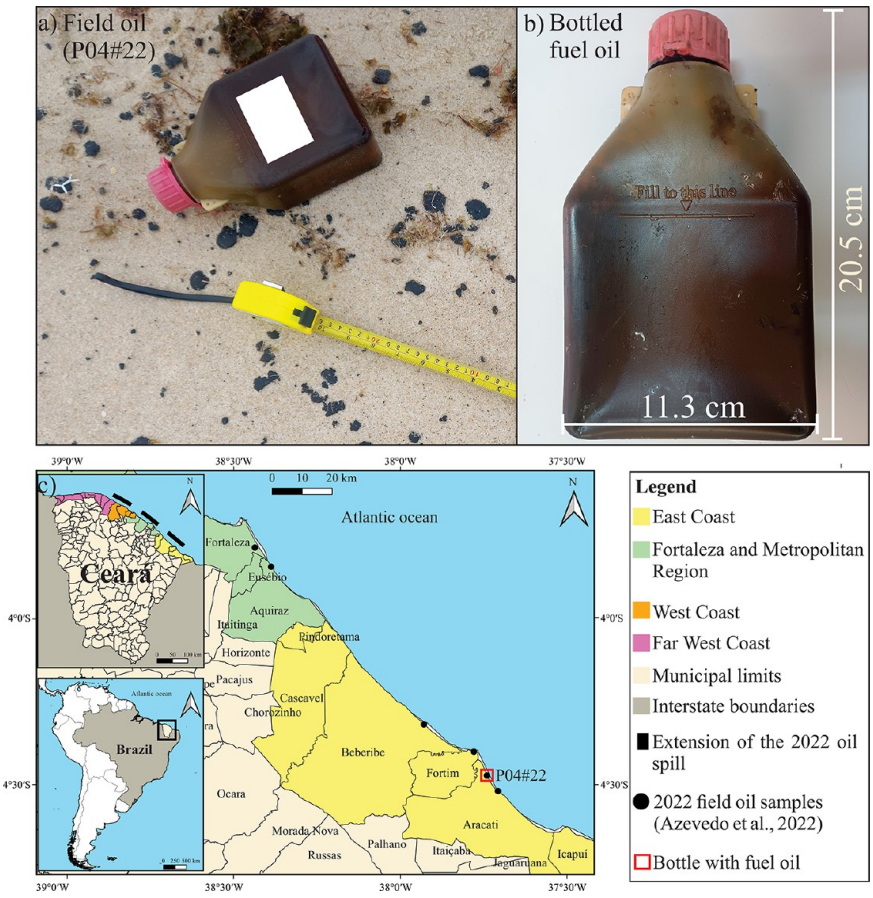

Figure 1. (a) Pictures of the fuel oil bottle and field oil stains stranded in Cumbe Beach right before their collection in January 2022. (b) Picture of the plastic fuel oil bottle showing its dimensions (20.5 × 11.3 × 6.7 cm), with 10.5 cm to the fill line. (c) Location where the bottle with the Fuel Oil Sample (FOS) and the field oil sample (P04#22) were collected in a coastal zone of Cumbe Beach, municipality of Aracati, state of Ceará, Northeast Brazil. It also presented the extension of 342 km affected by the 2022 oil spill,[17] including all four regions of Ceará (East Coast, Fortaleza and Metropolitan Region, West Coast, and Far West Coast) and other locations where field oil samples, which correlate with P04#22 sample, were collected and assessed by Azevedo et al.[6] Map reproduced with permission from Azevedo et al.[6]Copyright 2022 Elsevier.

with 11.6 m^3 of oil collected over an extension of approximately 342 km.[6,17] It affected 15 marine protected areas (MPAs), more than in the 2019 event.[17] Soares et al.[17] suggested that its source was within the Ceará shelf region or under the influence of the surface South Equatorial Current (SEC). Previous forensic geochemical studies showed that the January 2022 oil does not share the same source as the 2019 oil spill in Brazil[6] or the other three events afterward.[8,10,11,18] These mysterious events are usually related to foreign crude or fuel oils caused by intentional or accidental discharge from oil tankers, a global environmental problem.[19] While most of the previous events remain unsolved, this work presents new evidence for the source of the January 2022 oil spill: a fuel oil bottle half-filled with oil, containing small inorganic particles (<300 μm), and labeled with a foreign marine bunker company, which contaminatingly arrived with the 2022 spilled oil. This is the first report of a bottled oil co-occurring with an oil spill.

The northeast of Brazil is bathed by the South Atlantic Ocean, part of the global maritime transportation routes of oil tankers.[5,10] They usually transport crude oil and refined products and are powered by fuel oil, which can eventually be dumped into the sea.[20−22] Spills of fuel oils are more frequent than crude oils and are attributed to accidental and intentional releases at sea, shipboard fires, and collisions with the seafloor or permanent objects.[23] Heavy fuel oils (HFOs), the heavy residual part of the crude oil refining and cracking processes, are the most used commercial marine fuel oils, called bunker oils.[24−26] In January 2020, to reduce harmful emissions of sulfur oxides, a new Global Sulfur Cap regulation was implemented (IMO/MARPOL convention, Annex VI).[23,27,28] The residual fuels, termed "Very Low Sulfur Fuel Oil" (VLSFO), replace traditional intermediate fuel oils (IFOs) or HFOs, e.g., IFO 180 and IFO 380, with sulfur contents of up to 3.5% reduced to less than 0.5%.

Ships may continue to burn high sulfur fuels if equipped with exhaust gas cleaning systems (EGCS or scrubbers).[27] As a consequence, the number of ships with scrubbers in the international shipping fleet increased from 243 in 2015 to more than 4300 in 2020.[29] However, studies showed that scrubber water, which in most cases is discharged back to the sea, can have high concentrations of polycyclic aromatic hydrocarbons (PAHs) and heavy metals and increase water toxicity in aquatic ecosystems.[29,30] Considering this, the Pacific Environment organization released a new report in January 2025, recommending that the IMO ban scrubber discharge.[31]

This study applied forensic geochemistry using an extensive range of analytical techniques, including gas chromatography with flame ionization detector and coupled to mass spectrometry (GC-FID and GC-MS), comprehensive two-

https://doi.org/10.1021/acs.energyfuels.5c01581
Energy Fuels 2025, 39, 14254−14265

dimensional gas chromatography (GC × GC-FID), ultrahigh-resolution Fourier transform ion cyclotron resonance mass spectrometry (FT-ICR MS), and elemental analysis, to investigate an oil found in a specifically designed fuel plastic bottle stranded on the coast of Northeast Brazil in early 2022. The aim was also to characterize the bottled oil and determine whether it shares the same source as a spilled oil sample collected on the same day and at the same beach.

MATERIALS AND METHODS

Sample Set. The fuel oil sample (FOS) was removed from an unsealed plastic bottle, which was half filled (Figure 1a,b) and collected on January 28, 2022, in a coastal zone of Cumbe Beach on the east coast of Ceará, Northeastern Brazil (Figure 1c and Table S1). The bottle has a legible label of a foreign marine bunker company, a rectangular shape, a 750 mL capacity, a fill line, tamper-evident seals on the shoulder of the bottle and cap, and a red cap (Figures 1b and Figure S1). Flasks of similar size and shape are specifically designed and sold as sample bottles used by oil tankers for marine fuel testing and sample analysis, enabling the storage, transportation, and retention of fuel samples.[32] A field oil sample from the early 2022 oil spill collected on the same beach and the same day, labeled P04#22 (Figure 1a,c and Table S1) and previously investigated by Azevedo et al.,[6] was compared to the FOS. Both samples were collected soon after their arrival on Cumbe Beach.

According to Regulation 18 of MARPOL Annex VI, which controls the quality and availability of fuel for ships and controls fuel suppliers, ships need to retain on a board bunker delivery note (BDN) accompanied by a representative sample of a minimum of 400 mL fuel oil[33] such as the plastic bottle with oil investigated in this work (Figure 1a,b and Figure S1). In the more recent update, from March 2024, they recommend that the test samples be at least 600 mL.[34]

Oil Extraction and Separation. For the GC-FID analyses, 0.8 g of the FO and field oil (P04#22) samples were dissolved in 10 mL of *n*-hexane using a vortex (30 s) and then centrifuged at 3000 rpm (5 min). Then, 200 μL of the maltene dissolved in *n*-hexane was transferred to a vial, and the surrogate perdeuterated standard (SS) triacontane ($C_{30}D_{62}$) was added. The maltene was fractionated using a column with a 12 mm diameter containing 3.0 g of silica and 1 cm of sodium sulfate. The saturated fraction was eluted with 12 mL of *n*-hexane, and the perdeuterated tetracosane ($C_{24}D_{50}$) internal standard (IS) was added to the fractions. This experimental procedure was based on Wang et al.[26] The recoveries for the surrogate were 110 and 93% for the FO and P04#22 samples, respectively, which are within the recommendations (60−120%).[26]

For the GC-MS analyses, 0.6 g of the FO and field oil (P04#22) samples was dissolved, extracted five times with 6 mL of dichloromethane, and dried. In the next step, 12 mL of *n*-hexane was added to approximately 300 mg of the total oil extracted, which was centrifuged at 2000 rpm for 5 min to break the stability of the resin colloids and asphaltenes dispersed in the oil sample. This step was repeated five times, and all the samples were dried. Approximately 40 mg of the dry extract samples were used for fractionation. The fraction of saturated compounds (F1) was eluted using 30 mL of *n*-hexane. The aromatic fraction (F2) was eluted using 30 mL of a mixture containing *n*-hexane and dichloromethane (8:2), and the resin fraction (F3) was eluted using 30 mL of a mixture of dichloromethane and methanol (9:1). The internal standard pyrene-*d*10 at a 5.9 μg mL^{-1} concentration was used for the semiquantification of the PAHs (according to Martins et al.[10] and Nascimento et al.[11]).

GC-FID and GC-MS. The saturated fraction was analyzed using a GC-FID Shimadzu model GC 17-A. The *n*-alkanes and isoprenoids were analyzed using a capillary column (ELITE-1 100% dimethyl polysiloxane; 25 m × 0.20 mm × 0.33 μm). The following chromatographic conditions were used: carrier gas, hydrogen (H_2; 1.5 mL min^{-1}); injection mode, splitless; and injector temperature and detector temperature, 200 and 300 °C, respectively. The temperature program was 70 °C for 7 min and a heating rate of 6 °C min^{-1} to 300 °C, remaining constant for 15 min (details in Azevedo et al.[6]).

The saturated and aromatic fractions were analyzed using an Agilent Technologies 5973 quadrupole mass spectrometer coupled to a gas chromatograph. The target compounds and ions are listed in Table S2. One microliter of the fractions was injected into a 300 °C splitless injector with a purge time of 0.8 min. The analysis of saturated and aromatic hydrocarbon fractions was performed using a capillary column (HP 5MS; 5% phenyl−95% methylsiloxane, 30 m × 0.25 mm × 0.25 μm, details in Nascimento et al.[11]), with helium used as the carrier gas at a constant flow of 1.0 mL min^{-1}. The diagnostic ratios were calculated by using peak areas from the chromatograms.

The temperature program for saturated fractions was as follows: 60 °C for 2 min followed by a 22 °C min^{-1} ramp until 200 °C (held for 3 min) and a 3 °C min^{-1} ramp to 300 °C, with a 25 min isotherm. For the aromatic fractions, the oven program was as follows: 70 °C for 1 min followed by a ramp of 22 °C min^{-1} increase to 110 °C (held for 1 min), then to 200 °C at 1.5 °C min^{-1}, and finally to 300 °C at 3 °C min^{-1}, with a 10 min isotherm. For the saturated and aromatic hydrocarbons, the MS operated in the full scan (50−550 Da) and selected ion monitoring (SIM) mode, and compound identification was performed by comparison with published reference mass spectra (details in Martins et al.[10]).

The target biomarkers were the terpanes, steranes, diasteranes, and C30 tetracyclic polyprenoids (TPPs) in the saturated fraction and the triaromatic steranes in the aromatic fraction. The parental and the homologous methylated series of the conventional PAHs were also analyzed in addition to dibenzothiophene and its alkylated series and other PAHs with two to six rings.

GC × GC-FID. The whole FO and P04#22 samples were analyzed by GC × GC-FID to monitor the steranes, diasteranes, tricyclic and tetracyclic terpanes, hopanes, triaromatic steranes, and benzohopanes. The peaks were identified based on retention time in both dimensions and mass spectra from the GC × GC-HRT using pure standards, mass spectral matches (above 80% similarity; NIST/EPA/NIH 05 Mass Spectral Library), or mass spectral interpretation.[3,6]

One microliter aliquots of each sample were injected into a 310 °C splitless injector with a purge time of 0.5 min. The first-dimension analyses were carried out using a Restek Rxi-1 ms (59 m × 0.25 mm × 0.25 μm) column, and the second-dimension column was carried out using a 50% phenyl polysilphenylene-siloxane (SGE BPX50, 1.25 m × 0.10 mm × 0.1 μm). The first-dimension column and the dual-stage cryogenic modulator reside in the main oven, and the second-dimension column is in a separate oven, allowing for independent temperature control of the components. For the main oven, the temperature program was isothermal at 65 °C for 12.50 min followed by a ramp from 65 to 340 °C at 1.25 °C min^{-1}. The second-dimension oven was programmed to remain isothermal at 70 °C for 12.50 min followed by a ramp from 70 to 345 °C at 1.25 °C min^{-1}. The hot jet pulse width was 1.00 s, and the modulation period was 6.50 s with a 2.25 s cooling period between stages (details in Reddy et al.[3] and Azevedo et al.[6]).

FT-ICR MS. The FOS was analyzed by a 7 T Bruker SolariX 2xR FT ICRMS instrument (Bruker Daltonics GmbH, Bremen, Germany) tuned using NaTFA from *m*/*z* 107 to 2000. The mass spectra were operated in quadrupolar detection with a 0.010 ion accumulation time and collected in magnitude mode. To improve the experimental signal/noise ratio (S/N), 300 transients of 8 million points in the time domain were collected and summed. The sample concentration was 0.5 mg mL^{-1}, using a mixture of toluene/methanol (50:50) to dilute all samples. In ESI(−), a 5% ammonium hydroxide solution was added to support deprotonation. Moreover, in ESI(+), a 5% formic acid was added to assist in protonation.[35] Samples were infused into the ESI source by using a syringe pump set to deliver 240 μL h^{-1}. The capillary voltage and nebulizer gas pressure were adjusted to ±4.5 kV and 1.3 bar.

The Data Analysis 4.2 software (Bruker Daltonics GmbH, Bremen, Germany) was used to internally calibrate the homologous series of neutral nitrogen compounds (CcHhN1) for ESI(−) and the homologous series of basic nitrogen compounds (CcHhN1) for

https://doi.org/10.1021/acs.energyfuels.5c01581
Energy Fuels 2025, 39, 14254−14265

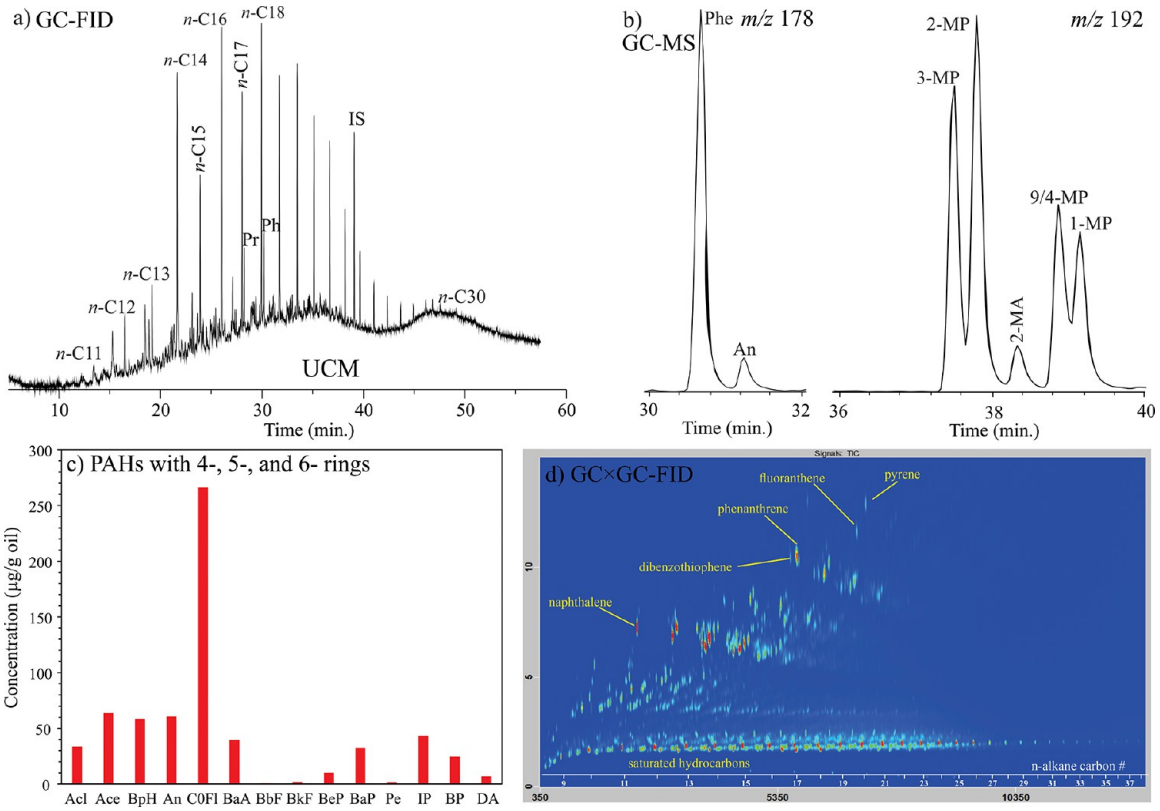

Figure 2. (a) GC-FID chromatogram of the Fuel Oil Sample (FOS). (b) *m/z* 178 and 192 chromatograms, from GC-MS analysis of aromatic fractions of the FOS, showing the presence of the phenanthrene (Phe), anthracene (An), methyl phenanthrenes isomers (MP), and 2-methylanthracene (2-MA) detected in the FOS. (c) Semiquantification of the PAHs acenaphthylene (Acl), acenaphthene (Ace), biphenyl (BpH), anthracene (An), benz[*a*]anthracene (BaA), benzo[*b*]fluoranthene (BbF), benzo[*k*]fluoranthene (BkF), benzo[*e*]pyrene (BeP), benzo[*a*]pyrene (BaP), perylene (Pe), indeno[1,2,3-*cd*]pyrene (IP), dibenzo[*g,h,i*]perylene (BP), and dibenz[*a,h*]anthracene (DA) for the FOS collected on the state of Ceará in January 2022. (d) GC × GC-FID plane view chromatogram showing a full series of saturates and aromatic compounds in the FOS.

ESI(+). The software Composer 1.0.6 (Sierra Analytics, Modesto, CA, USA) was used to process the mass spectra to assign molecular formulas with a mass accuracy below 0.7 ppm (details in Lima et al.[35]).

CHNS Elemental Analysis. The FOS was analyzed twice for bulk carbon, hydrogen, and nitrogen and once for sulfur by Midwest Microlab (Indianapolis, Indiana).[3] For the first CHN analysis, an aliquot of the neat oil (~5 mg) was added to a tin capsule, crushed, and analyzed by an Exeter CE440 CHN analyzer. For the second analysis, the combustion aid, vanadium pentoxide, was added, and the combustion time was extended by 15 s. The sulfur content was determined by a Schoniger combustion.

Microscopic Analysis. A digital microscope and a Hitachi TM3000 tabletop microscope were used to analyze the particles present in the FOS, and an energy-dispersive X-ray spectroscope was used to visualize the particles of aluminum and silicon.

RESULTS AND DISCUSSION

Fuel Oil Investigation. The oil in the fuel sampling bottle is a viscous liquid with a dark brown color (Figure S2a), characteristic of crude and heavy fuel oils;[36−38] has a burnt smell; and contains many visible small solid particles (Figure S2b). A detailed assessment of the chemical composition of bottled oil was performed to assess its fuel characteristics and properties. For this, a combination of multiple analytical techniques was employed, including GC-FID, GC-MS, GC × GC-FID, and ESI(±) FT-ICR MS, in addition to CHNS elemental analysis and microscopy imaging, as similarly applied before for the Brazilian 2019 oil spill[3,35] but for the first time for samples related to the 2022 oil spill in Ceará.

GC-FID Profile. The GC-FID fingerprint of the FOS presents a high and bimodal unresolved complex mixture (UCM) and a wide carbon range from *n*-C_{11} to *n*-C_{30} (Figure 2a), which are characteristics of blended oils used as fuel.[39−41] This profile can also indicate a mixture of biodegraded crude oil with light-recharged oil in the reservoir.[42] However, the detection of 25-norhopanes, common in extensively biodegraded oils,[43] in low abundance and the high values of the *n*-C_{17}/pristane (2.60) and *n*-C_{18}/phytane (2.67) ratios indicate that the biodegradation was not extensive.

GC-MS Profile. The FOS has a full range of biomarkers, such as terpanes, steranes, diasteranes, C_{30} tetracyclic polyprenoids (TPPs), and triaromatic steranes (Figure S3). Also present were the parent and alkylated PAHs, including the naphthalenes, phenanthrenes, dibenzothiophenes, fluorenes, and chrysenes (Figure S4; concentration in Figure S5). Alkylated PAHs were more abundant than the parent PAHs (Figure S5), a typical feature of petroleum[3] that was already observed in other spilled oils that reached the Brazilian coastline in recent years.[10,35] This profile is consistent with crude and refined oils, especially HFOs, which can sometimes be confused since they share some physical properties, chromatographic features, and chemical composition.[25,44,45]

The distribution and relative abundance of PAHs in the FOS are indicative of thermal alteration from refining. The 2- and 3-methylphenanthrene (MP) isomers, which are more thermally stable and found in greater abundance in refined products,[25,40] are more abundant than the 9/4-MP and 1-MP in the FOS

https://doi.org/10.1021/acs.energyfuels.5c01581
Energy Fuels 2025, 39, 14254−14265

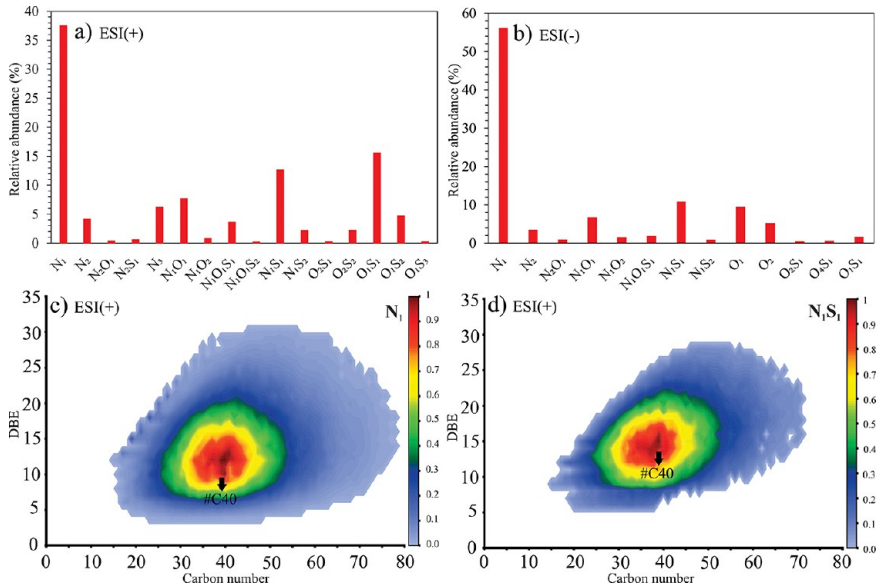

Figure 3. Heteroatom class distributions obtained by (a) ESI(+) FT-ICR MS and (b) ESI(−) FT-ICR MS for the FOS collected in the state of Ceará, Brazil, in early 2022. Isoabundance contoured plots of the double bond equivalent (DBE) vs carbon number for the classes (c) N_1 and (d) N_1S_1, obtained from ESI(+) FT-ICR MS analysis of the FOS.

(Figure 2b). In addition, anthracene (An) and 2-methylanthracene (2-MA), which are formed during rapid heating and cooling in some refining processes, such as cracking, and are usually absent or detected in very low abundance in crude oils,[25,46,47] are detected in the FOS (Figure 2b). The plots of the 2-MA/ΣMP vs (3- + 2-MP)/(9/4- + 1-MP) ratios (Figure S6a) and An/(An + Phe) vs (3- + 2-MP)/(9/4- + 1-MP) ratios (Figure S6b) illustrate that the FOS has the characteristic of HFOs (Table S3).[45]

The measurable concentration of PAHs with four, five, and six rings in the FOS (Figure 2c), including fluoranthene, benzofluoranthene, benzopyrene, indeno[1,2,3-*c,d*]pyrene, dibenzo[*a,h*]anthracene, and benzo[*g,h,i*]perylene, which are rarely found in crude oils, is also consistent with fuel oil.[26] These compounds can be produced during the distillation process of the residue or production of any cracked gas oil cutter stock, or they can be concentrated within the distillate residue.[26] The pyrogenic index ∑(other 3−6 ring PAHs)/∑(5 alkylated PAH series) (Table S3) and the 2 + 3-MDT/4-MDT ratio with the value of approximately one (Table S3) corroborate that the FOS is a bunker-type fuel (Figure S7).[48,49]

GC × GC Profile. The FOS is rich in compound classes such as saturates, PAHs, and biomarkers (Figure 2d and Figure S8). The GC × GC-FID high peak resolution reveals that the FOS presents a bimodal profile with the *n*-C12 to *n*-C28 alkanes detected in high abundance and the high-molecular-weight *n*-alkanes (*n*-C30 to *n*-C38; Figure S8b) detected in low abundance. In addition, the FOS is rich in naphthalenes, including the parent (C0N) and its alkylated analogs (e.g., C1N and C2N; Figure 2d and Figure S8a). These volatile compounds were detected in low abundance using GC-MS (Figure S5a), likely due to their loss during the extraction, concentration, and fractioning of the oil, which were not applied in GC x GC-FID since an extract of the whole oil was analyzed. Hence, the FOS has the contribution of fresh oil richer in volatile compounds (Figure 2d and Figure S8a).

The predominance of the more alkylated naphthalenes (C3N and C4N; Figure 2d and Figure S5a) and the C2D/C2P (0.69) and C3D/C3P Phen (0.34) ratios calculated using the GC-MS corroborates that the FOS can be an IFO, probably an IFO 380 rich in naphthalenes, a lighter form of HFO and one of the most used groups of marine HFOs.[25,50] Blending lighter gas oil or other cutter stocks with residuum distillation is a common practice to control the viscosity of HFOs.[25,51] A high abundance of the low-molecular-weight *n*-alkanes up to *n*-C17 and the high abundance of the naphthalenes suggest that naphtha was the light fraction used in the blend.[52,53]

FT-ICR MS Analysis. The ESI(+) and ESI(−) mass spectra for FOS are presented in Figure S9. The ESI(+) heteroatom class distribution showed that the FOS has a higher number of sulfur-containing classes (Figure 3a and Table S4), with O_1S_1 (15.7%) and N_1S_1 (12.7%) the second and third most abundant after the N_1 class (pyridine species),[54] summing 42.9% of the total relative abundance classes. The ESI(−) heteroatom class distribution presents six sulfur-containing classes (Figure 3b and Table S4), with a higher abundance of N_1S_1 (10.9%) followed by $N_1O_1S_1$, O_1S_1, N_1S_2, O_4S_1, and O_2S_1, summing 16.6% of the total relative abundance classes. These results indicate that the fuel oil is rich in sulfur content. The presence of sulfur compounds in high abundance was similarly observed by Reddy et al.[3] in the ESI(±) FT-ICR MS analysis of the Brazilian 2019 oil spill, which was also a heavy fuel oil with a high sulfur content (3.6%). In addition, the overall H/C ratios for the acidic and basic polar composition of the FOS were 1.22 and 1.44, respectively, values that agree with the literature for oil samples.[54,57]

The high abundance in #C = 40 observed for the N_1 class assessed by ESI(+) (Figure 3c) supports a residue from atmospheric distillation since Dalmaschio et al.[55] observed that the maximum abundance migrated from #C = 35 in crude oil to #C = 40 in atmospheric distillation residue with a boiling point >372.9 °C, close to the initial boiling point of the residuum of ∼375 °C observed by Reddy et al.[3] in the oil sample from the 2019 oil spill. Furthermore, a high abundance of elevated values of carbon numbers was also observed for the N_1S_1 (Figure 3d), N_2, N_1O_1, and O_1S_1 classes of basic polar

https://doi.org/10.1021/acs.energyfuels.5c01581
Energy Fuels 2025, 39, 14254−14265

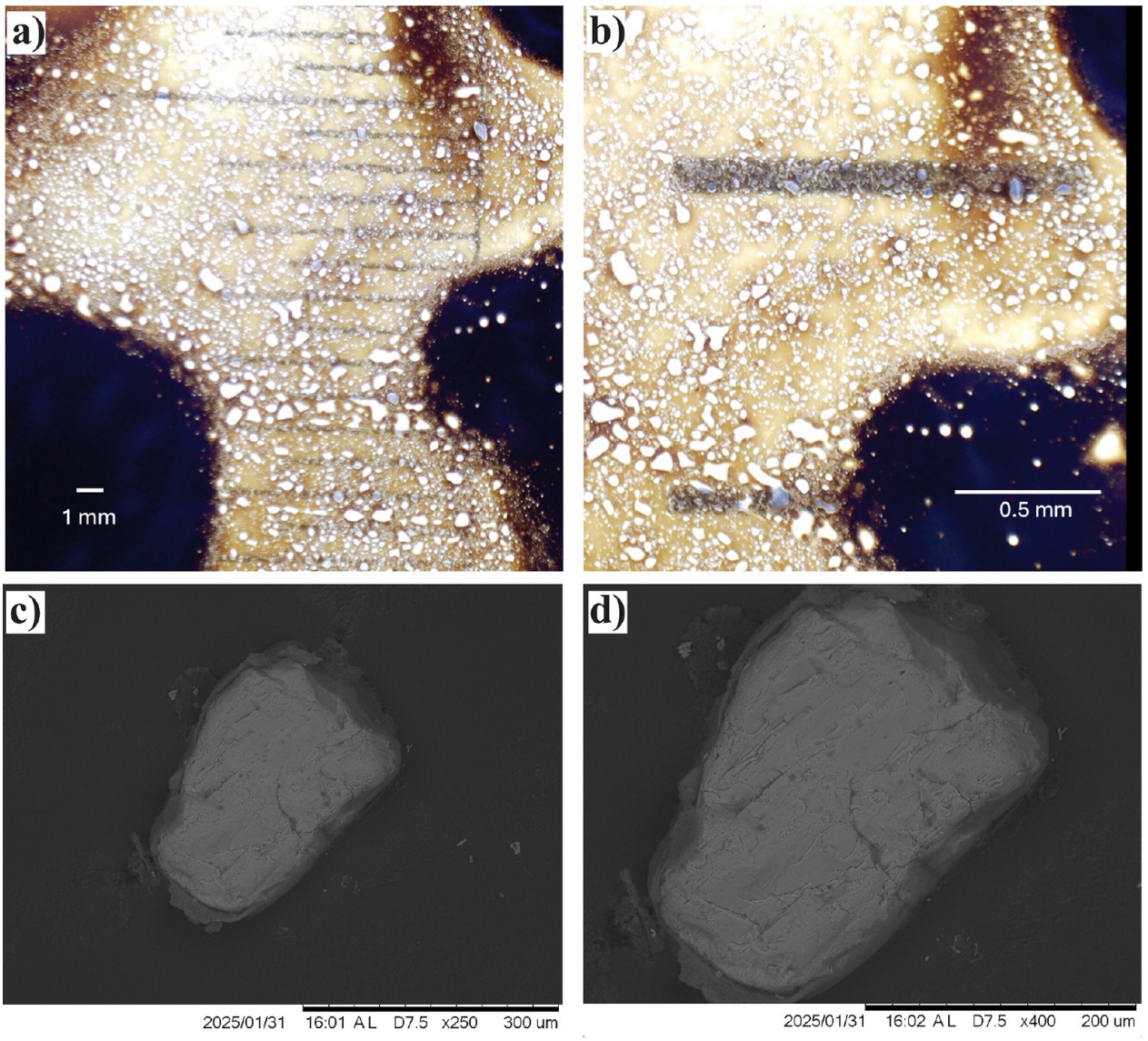

Figure 4. Analysis of particulate material in the FOS with a digital microscope: (a) image with 1 mm resolution and (b) image with 0.5 mm resolution. Analysis of particulate material in the FOS was performed with a Hitachi TM3000 tabletop microscope. Backscattered electron image of a single particle in the FOS: (c) image with 300 μm resolution and (d) image with 200 μm resolution. Aluminum and silicon were detected with energy-dispersive X-ray spectroscopy.

compounds (Figure S10). This can be due to the increasing distillation temperature accompanied by an increase in carbon number and DBE values.[56,57]

Bulk C, H, N, and S. The bulk C, H, N, and S contents in the FOS were initially measured by Midwest Microlabs to be 54.8, 10.1, 0.40, and 2.44% of the oil mass, respectively. While the H, N, and S contents were reasonable for crude and fuel oils, the carbon content was unusually lower than expected, 85%,[3,58] unlike what was observed by FT-ICR MS through the H/C ratio. Results in previous analyses of petroleum for C and H by Midwest Microlabs were ~86 and ~10.5% (Table S5).[3,59−62] The FOS was reanalyzed with a combustion aid, vanadium pentoxide, and a longer combustion time, and a similar result was obtained (56.8% C and 10.2% H). Ethanol is the only known fuel with similar C and H contents (52.1% C and 13.2% H). No other chromatographic and mass spectral evidence supports the low C content.

The FOS presents a high sulfur content (2.44%; Table S5), which agrees with the high abundance of sulfur compounds (benzothiophenes and dibenzothiophenes; Figure 2d) and several sulfur classes (Figure 3a,b and Table S4). This sulfur content is higher than the values recommended in the 2020 regulation (<0.5%) and can be used only by ships with scrubbers (IMO/MARPOL convention, Annex VI).[27] The high sulfur content may explain the release of the oil into the environment.

Microscopic Analysis. Many small nonmagnetic solid particles were observed in the fuel oil sample (Figure S2b), typical of catalyst fines (cat fines) frequently found in HFOs.[63,64] This is unusual, as cat fines are typically used to reduce the sulfur content of fuel oils.[64] Microscopic analysis indicates that these solids are rich in Al and Si, consistent with cat fines (Figure 4).[63,64] They also have variable micrometric sizes and shapes typical of cat fines (Figure 4), consisting of large particles and jagged, smaller fragments.[64] These particles are aluminosilicate zeolite catalysts utilized in the oil cracking process at refineries.[63,65] The considerable amount of these

https://doi.org/10.1021/acs.energyfuels.5c01581
Energy Fuels 2025, 39, 14254−14265

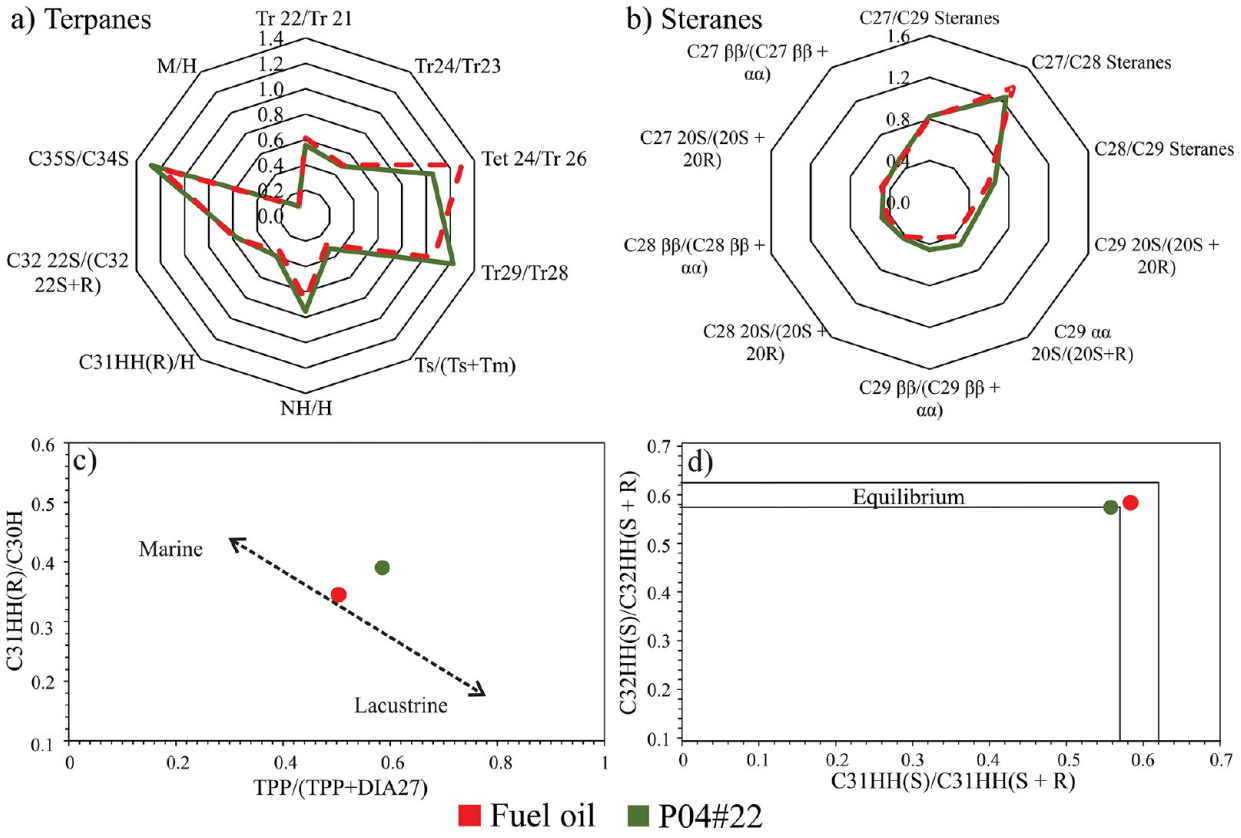

Figure 5. Radar plots comparing the diagnostic ratios derived from the (a) terpanes and (b) steranes assessed by GC-MS of the FOS and the P04#22 sample collected in early 2022 at Ceará, Brazil. Plots to assess the depositional environment and maturity of the FOS and the P04#22 sample.[72−77] (c) TPP/(TPP + DIA27) vs C31HH(R)/C30H. (d) C31HH(S)/C31HH(S + R) vs C32HH(S)/C32HH(S + R).

catalytic fines (Figure S2b) can be responsible for the unusually lower carbon content of the FOS.

Cat fines are not typical wear but can quickly create enormous problems for the ships. They can cause rapid wear in marine engines during combustion[63,64] and damage the engine by wearing down the injection and pump.[66] The accepted limit varies between 7 and 15 mg kg^{-1}, depending on the engine specifications, and metal particles can be found in the oil even after the extraction process.[65] Therefore, their undesirable presence may be another explanation for oil dumping in the ocean.

In addition to the marine engine issues, the particles of the catalytic fines, mainly Al, Si, and O, which are in the oxidic form Al_2O_3 and SiO_2,[63,64] can provoke environmental and human health problems.[66−68] Their release and accumulation in the aquatic environment cause adverse effects on organisms, including microbes, algae, fish, and invertebrates.[67] Hence, cat fines released from oil pills or chronic releases of bunker oils may pose an additional potential threat to marine and coastal environments.

Correlation with the Early 2022 Oil Spill. A geochemical correlation was verified between the FO and P04#22 samples, which arrived at the same beach area and at relatively the same time. As the Brazilian coast is constantly impacted by oil residues and plastics dumped in the South Atlantic Ocean and carried by oceanic currents,[5,10,69] the oil from the plastic bottle and the spilled oil could potentially have distinct sources.

Floating objects likely associated with spilled oils were already reported in the literature, as related to the Deepwater Horizon disaster, which traveled at the same speed and relative heading and were found in the Gulf of Mexico surface waters and along coastal beaches shortly after the explosion of Deepwater Horizon.[70] These buoyant materials can provide evidence for the origin and fate of spilled oils, such as the plastic bottle with the fuel oil (FO) investigated herein. It is worth emphasizing that this is the first record of a bottle filled with oil, which is designed for fuel testing and labeled with a marine bunker company, co-occurring with an orphan oil spill.

The P04#22 sample was previously investigated by Azevedo et al.,[6] showing its correlation with five other spilled oil samples collected on five distinct beaches over an extension of ∼130 km along the eastern coast of the Ceará, where the oil arrived first in late January, and the noncorrelation with the Brazilian 2019 oil spill, despite both being high-sulfur HFOs. The spilled oil then drifted westward, extending to new sites until mid-February over a length of ∼342 km and reaching 84 beaches.[17]

The FO and P04#22 samples exhibit similar GC-FID profiles, characterized by a high and bimodal UCM, as well as midchain *n*-alkanes (*n*-C17 to *n*-C28) in higher abundance (Figure S11). The *n*-alkanes with low molecular weight (<*n*-C16) are only detected in the FOS. The bottle probably protected the FOS from exposure to weathering processes, such as evaporation, and was capped, preserving the more volatile compounds.[50,71]

Biomarker analysis by GC-MS supported that FO and P04#22 samples have the same source since they share similarities in their *m*/*z* 191 (tricyclic, tetracyclic, and pentacyclic terpanes; Figure S3) and *m*/*z* 217 profiles

https://doi.org/10.1021/acs.energyfuels.5c01581
Energy Fuels 2025, 39, 14254−14265

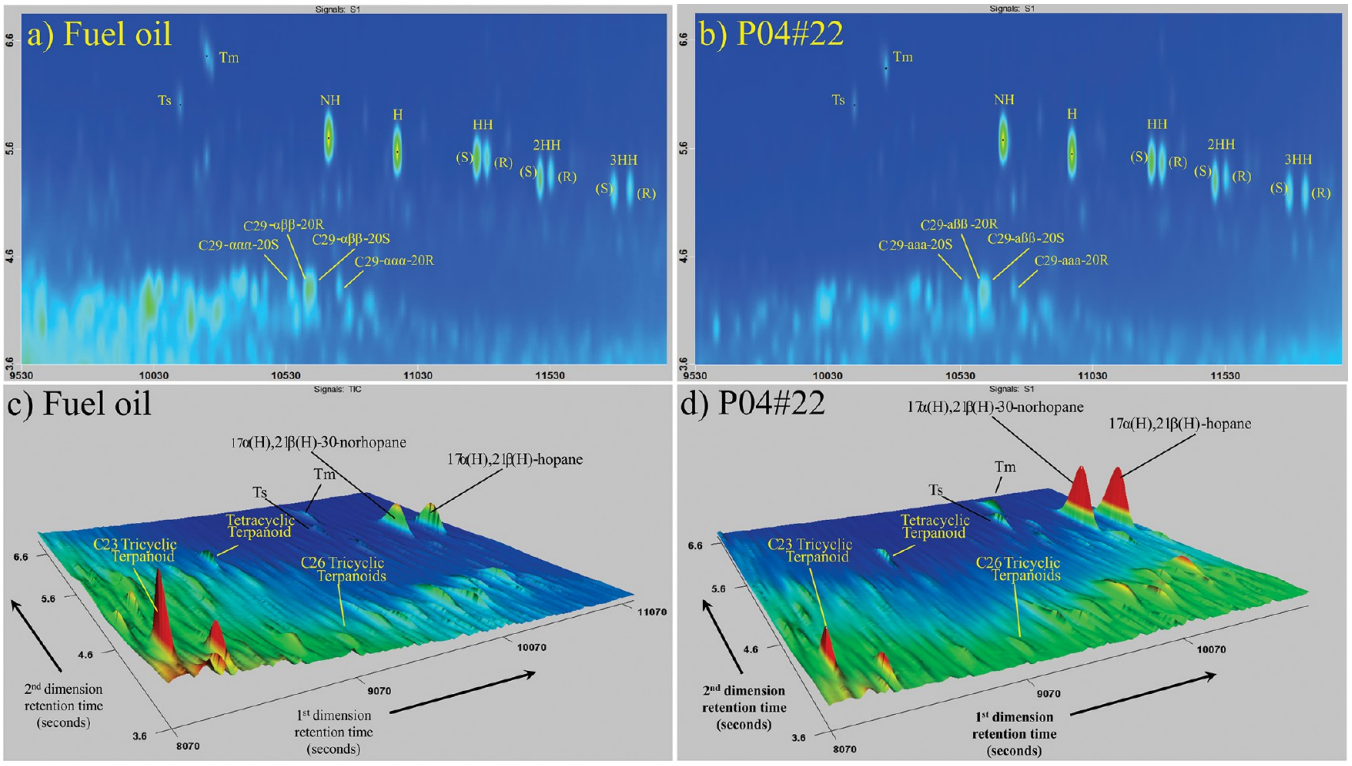

Figure 6. GC × GC-FID plane view chromatograms showing the series of hopanes and steranes for the (a) FOS and (b) P04#22 sample. GC × GC-FID mountain plot chromatograms showing the full series of the terpanes for the (c) FOS and (d) P04#22 sample. Sample P04#22 was previously assessed using GC × GC-FID by Azevedo et al.[6]

(steranes; Figure S3). The main difference is in the abundance of the less resistant tricyclic terpanes. Among the tricyclic terpanes, C23 tricyclic (Tr 23) is the most abundant in both samples (Figure S3). The distribution of the C24 tetracyclic (Tet 24) and the isomers S and R of the C26 tricyclic (Tr 26) is also similar in the FOS and in the P04#22 sample, with the Tet 24 present in higher abundance than the isomers of Tr 26 (Figure S3). In the hopane profile, the C30 17α(H), 21β(H)-hopane (H) is present in higher abundance than the C29 17α(H), 21β(H)-hopane (NH; Figure S3), and the C27 17α(H) trisnorhopane (Tm) is in higher abundance than the C27 18α(H) trisnorneohopane (Ts; Figure S3). C27 $\alpha\beta\beta$(R), C28 $\alpha\beta\beta$(R), and C29 $\alpha\beta\beta$(R) presented the highest abundance in the C27, C28, and C29 sterane profiles, respectively, in addition to the identification of C30 steranes in both samples (Figure S3). They also have similarities in the diasteranes (m/z 259, Figure S3) and the triaromatic steranes profiles (m/z 231, Figure S3). The diagnostic ratios based on the resistant terpanes and steranes better display their similarity (Figure 5a,b and Tables S6 and S7).

The comparable geological genesis between the FOS and P04#22 sample reinforces their correlation. The plots using tricyclic terpanes and hopanes (Figure S12a–c and Table S8) suggest that they were generated from marl or marine carbonate source rocks.[72] The low values for the regular steranes/17α-hopanes ratio (Table S8) indicate a terrigenous and microbially reworked organic matter.[73] The plot between the TPP/(TPP + 27 Dia) and the C31HH(R)/C30H ratios (Figure 5c and Table S8) and the presence of the C30 steranes (Figure S3) support a marine carbonate depositional environment for their source rock.[72,74,75] Furthermore, the geochemical parameters based on the biological and geological isomers of hopanes and steranes indicate that they reached the oil generation window (Figure 5d, Figure S12d, and Table S8).[72,76,77]

The GC × GC-FID results corroborate the similarities between the FO and P04#22 samples, mainly in the profile of the hopanes and steranes (Figure 6). Similar to the observation in the biomarker profiles assessed by GC-MS, GC × GC-FID showed that the isomer Tm is in higher abundance than the Ts and C30 17α(H), 21β(H)-hopane (H) has similar abundance as the C29 17α(H), 21β(H)-hopane (NH, norhopane; Figure 6a,b), with the ratio NH/H close to 1 in both samples (Figure S13). For the homohopane profile, the isomer S is more abundant than R for the C31, C32, and C33 homohopanes (HH, 2HH, and 3HH, respectively; Figure 6a,b). For the steranes, C29 $\alpha\beta\beta$-20R and 20S are the predominant compounds (Figure 6a,b). The C23 tricyclic is also the most abundant among the tricyclic terpanes, and the C24 tetracyclic terpane was detected in both samples (Figure 6c,d).

In accordance with the GC-MS results, the GC × GC-FID analyses show differences between the FO and P04#22 samples concerning the tricyclic terpane profiles. The Tr23 is more abundant than C30H in the FOS, unlike that observed for the P04#22 sample (Figure 6c,d). Additionally, the ratios calculated using C23 and C26 tricyclic terpanes and the C30 17α(H), 21β(H)-hopane presented distinct values (Figure S13). Arekhi et al.[78] showed that the lower-molecular-weight tricyclic terpanes (Tr 21 to Tr 24) weathered rather rapidly during the initial months when the oil was floating over the ocean, which can explain the differences observed in the tricyclic terpanes. Nascimento et al.[11] also observed some differences in the tricyclic terpane profiles among the 16 waxy

https://doi.org/10.1021/acs.energyfuels.5c01581
Energy Fuels 2025, 39, 14254−14265

tarball samples that affected the Northeast coast of Brazil in late 2022 and attributed that to the weathering process.

In addition, the GC × GC-FID results showed additional differences in the chromatographic profile for the P04#22 sample, with the absence of low- and medium-molecular-mass compounds (Figure S14), which is explained by weathering processes. Considering that the FO and P04#22 samples share the same source, as shown by the recalcitrant biomarkers, it is estimated that there was a loss of 85% of GC-amenable compounds due to weathering. Another possibility for the compositional differences is that all the fuel oil on the offending ship is not homogeneous and originated from two different fuel tanks with different biomarker ratios, like what was observed in the Cosco Busan (2007) and the North Cape (1996) oil spills in 1996.[79,80]

Ultimately, the gas chromatography analysis by GC-FID, GC-MS, and GC × GC-FID showed strong evidence of the correlation between the early 2022 oil spill in Ceará and the bottled oil labeled with a foreign marine bunker company found during this event, which discloses for the first time that this oil spill is from an international tanker on the South Atlantic route. Furthermore, this geochemical approach reinforces the importance of using resistant biomarkers in forensic environment studies of oil spills, as they showed to be efficient in oil correlation even in weathered spilled oils exposed under tropical climate conditions,[35] such as the P04#22 sample, with a loss of 85% of GC-amenable compounds due to weathering processes.

The findings presented in this study reinforce the importance of searching for bottles, one of the most abundant types of debris in the ocean,[81,82] and other materials, such as plastitar (i.e., a mix of oil and plastic) and oiled floating objects,[70] when responding to future mysterious oil spills. The oil related to the materials can be used for geochemical correlations, and any information in the objects, such as company names, countries, and dates, can be useful in forensic investigations, following the same strategy as that applied in this work.

CONCLUSIONS

The comprehensive chemical assessment of bottled oil stranded on the Brazilian coast in January 2022 revealed a heavy fuel oil (HFO). The oil presents a GC-FID chromatogram with a bimodal UCM, which is similar to blended oils. The PAHs assessed by GC-MS are consistent with petroleum products that underwent heating processes. The GC × GC-FID analysis revealed that it is rich in light compounds, such as naphthalenes and low-molecular-weight *n*-alkanes. This profile suggests that naphtha was the light fraction used in the blended fuel oil, consistent with an IFO 380. Furthermore, the N_1, N_2, N_1O_1, N_1S_1, and O_1S_1 classes assessed by ESI(+) FT-ICR MS indicate that the heavy part of the bottled oil is from a residue obtained from atmospheric distillation.

The bottled fuel oil also has a high sulfur content (%S = 2.44). This type of high-sulfur fuel oil can be used only by vessels with scrubbers that control acid-gaseous emissions, although it generates toxic wastewater. It also has a significant amount of catalytic fines, which can cause rapid wear in marine engines during combustion. This is uncommon, as these fines are usually related to low-sulfur fuels. Additionally, these findings draw attention to the potentially harmful effects of cat fines released together with spilled fuel oils on marine and coastal environments and, consequently, on human health.

Forensic geochemistry using multiple gas chromatographic techniques indicated that the bottled oil and the P04#22 sample collected at the same beach and on the same day share the same source. Both samples present a bimodal UCM and have similarities in their recalcitrant biomarker profiles and geological genesis. Hence, this correlation discloses the origin of the 2022 oil spill on the Ceará coast, Brazil, from an international tanker on the South Atlantic routes.

The results presented in this work indicate that cleanup crews should search for oil bottles and other similar materials when responding to future mysterious oil spills, as they can provide evidence about the source of the spilled oil. Based on the beached bottle of fuel oil investigated herein, we hypothesized that the high sulfur content and the presence of catalytic fines could be the reason that the fuel oil was discharged into the sea.

ASSOCIATED CONTENT

Supporting Information

The Supporting Information is available free of charge at https://pubs.acs.org/doi/10.1021/acs.energyfuels.5c01581.

Sample information, list of target compounds assessed by GC-MS, diagnostic ratios and parameters based on the saturated and aromatic compounds, relative abundance of heteroatom classes assessed by FT-ICR MS, pictures of the plastic bottle and fuel oil, selected ion chromatograms obtained by GC-MS, GC-FID chromatograms, GC × GC-FID chromatograms, mass spectra from FT-ICR MS analysis, and additional graphs to provide more details of the results and improve discussions (PDF)

AUTHOR INFORMATION

Corresponding Authors

Christopher M. Reddy − *Department of Marine Chemistry and Geochemistry, Woods Hole Oceanographic Institution (WHOI), Woods Hole, Massachusetts 02543-1050, United States;* orcid.org/0000-0002-7814-2071; Email: creddy@whoi.edu

Rivelino M. Cavalcante − *Institute of Marine Sciences (LABOMAR), Federal University of Ceará (UFC), Fortaleza, Ceará 60165-081, Brazil*; Email: rivelino@ufc.br

André H. B. Oliveira − *Analytical Chemistry and Physical Chemistry Department (DCFQ), Federal University of Ceará (UFC), Fortaleza, Ceará 60440-900, Brazil; Institute of Marine Sciences (LABOMAR), Federal University of Ceará (UFC), Fortaleza, Ceará 60165-081, Brazil*; Email: andrehbo@ufc.br

Laercio L. Martins − *Institute of Marine Sciences (LABOMAR), Federal University of Ceará (UFC), Fortaleza, Ceará 60165-081, Brazil; Laboratory of Petroleum Engineering and Exploration (LENEP), North Fluminense State University (UENF), Macaé, Rio de Janeiro 27932-125, Brazil;* Present Address: Laboratory of Petroleum Engineering and Exploration (LENEP), North Fluminense State University (UENF), Macaé, Rio de Janeiro 27925-535, Brazil; orcid.org/0000-0001-6216-990X; Email: laercio@lenep.uenf.br

https://doi.org/10.1021/acs.energyfuels.5c01581
Energy Fuels 2025, 39, 14254−14265

Authors

Rufino Neto A. Azevedo − *Analytical Chemistry and Physical Chemistry Department (DCFQ), Federal University of Ceará (UFC), Fortaleza, Ceará 60440-900, Brazil*

Adriana P. Nascimento − *Institute of Marine Sciences (LABOMAR), Federal University of Ceará (UFC), Fortaleza, Ceará 60165-081, Brazil*

Vinícius B. Pereira − *Institute of Chemistry (IQ), Federal University of Rio de Janeiro (UFRJ), Rio de Janeiro 21941-909, Brazil;* orcid.org/0000-0001-8694-6793

Danielle M.M. Franco − *Chemistry Institute, Federal University of Goiás (UFG), Goiânia, Goiás 74.001-970, Brazil;* orcid.org/0000-0002-3691-4328

Robert K. Nelson − *Department of Marine Chemistry and Geochemistry, Woods Hole Oceanographic Institution (WHOI), Woods Hole, Massachusetts 02543-1050, United States;* orcid.org/0000-0003-0534-5801

Boniek Gontijo − *Chemistry Institute, Federal University of Goiás (UFG), Goiânia, Goiás 74.001-970, Brazil;* orcid.org/0000-0003-1197-4284

Débora A. Azevedo − *Institute of Chemistry (IQ), Federal University of Rio de Janeiro (UFRJ), Rio de Janeiro 21941-909, Brazil;* orcid.org/0000-0003-4924-6741

Ronaldo F. do Nascimento − *Analytical Chemistry and Physical Chemistry Department (DCFQ), Federal University of Ceará (UFC), Fortaleza, Ceará 60440-900, Brazil;* orcid.org/0000-0002-6393-6944

Complete contact information is available at: https://pubs.acs.org/10.1021/acs.energyfuels.5c01581

Author Contributions

The manuscript was written with contributions from all authors. All authors have approved the final version of the manuscript.

Funding

The Article Processing Charge for the publication of this research was funded by the Coordenacao de Aperfeicoamento de Pessoal de Nivel Superior (CAPES), Brazil (ROR identifier: 00x0ma614).

Notes

The authors declare no competing financial interest.

■ ACKNOWLEDGMENTS

This work was supported by the Federal University of Ceará (UFC, Brazil), North Fluminense State University (UENF, Brazil), Federal University of Goiás (UFG, Brazil), Federal University of Rio de Janeiro (UFRJ, Brazil), and the Wood Hole Oceanographic Institution (WHOI, EUA). LECO (St. Joseph, Michigan) graciously supports their GC × GC platforms. C.M.R. was supported by WHOI IRD 31001. C.M.R. thanks Frieder Klein and Grace Schwartz for their help with the microscopic analysis. L.L.M. thanks the Postgraduate Program in Tropical Marine Sciences (PPGCMT/LABOMAR-UFC) for the position of visiting professor (Public Notice no. 04/2022 published in the DOU on 01/17/2022) and the Fundação de Amparo à Pesquisa do Estado do Rio de Janeiro (FAPERJ, E-26/210.979/2024). R.M.C. thanks CNPq for the PQ-1 fellowship (314013/2023-7 and 440880/2020-3).

■ REFERENCES

(1) de Oliveira, O. M. C.; de S. Queiroz, A. F.; Cerqueira, J. R.; Soares, S. A. R.; Garcia, K. S.; Filho, A. P.; de L. da S. Rosa, M.; Suzart, C. M.; de L. Pinheiro, L.; Moreira, Í. T. A. Environmental disaster in the northeast coast of Brazil: Forensic geochemistry in the identification of the source of the oily material. *Mar. Pollut. Bull.* **2020**, *160*, No. 111597.

(2) Lira, A. L. d. O.; Craveiro, N.; da Silva, F. F.; Rosa Filho, J. S. Effects of contact with crude oil and its ingestion by the symbiotic polychaete Branchiosyllis living in sponges (Cinachyrella sp.) following the 2019 oil spill on the tropical coast of Brazil. *Sci. Total Environ.* **2021**, *801*, No. 149655.

(3) Reddy, C. M.; Nelson, R. K.; Hanke, U. M.; Cui, X.; Summons, R. E.; Valentine, D. L.; Rodgers, R. P.; Chacón-Patiño, M. L.; Niles, S. F.; Teixeira, C. E. P.; Bezerra, L. E. A.; Cavalcante, R. M.; Soares, M. O.; Oliveira, A. H. B.; White, H. K.; Swarthout, R. F.; Lemkau, K. L.; Radović, J. R. Synergy of Analytical Approaches Enables a Robust Assessment of the Brazil Mystery Oil Spill. *Energy Fuels* **2022**, *36*, 13688−13704.

(4) Soares, M. O.; Teixeira, C. E. P.; Bezerra, L. E. A.; Rabelo, E. F.; Castro, I. B.; Cavalcante, R. M. The most extensive oil spill registered in tropical oceans (Brazil): the balance sheet of a disaster. *Environ. Sci. Pollut. Res.* **2022**, *29*, 19869−19877.

(5) Zacharias, D. C.; Lemos, A. T.; Keramea, P.; Dantas, R. C.; da Rocha, R. P.; Crespo, N. M.; Sylaios, G.; Jovane, L.; da Silva Santos, I. G.; Montone, R. C.; de Oliveira Soares, M.; Lourenço, R. A. Offshore oil spills in Brazil: An extensive review and further development. *Mar. Pollut. Bull.* **2024**, *205*, No. 116663.

(6) Azevedo, R. N. A.; Bezerra, K. M. M.; Nascimento, R. F.; Nelson, R. K.; Reddy, C. M.; Nascimento, A. P.; Oliveira, A. H. B.; Martins, L. L.; Cavalcante, R. M. Is there a similarity between the 2019 and 2022 oil spills that occurred on the coast of Ceará (Northeast Brazil)? An analysis based on forensic environmental geochemistry. *Environ. Pollut.* **2022**, *315*, No. 120283.

(7) Bastos, L. P. H.; da Costa Cavalcante, D.; Alferes, C. L. F.; da Silva, D. B. N.; de Oliveira Ferreira, L.; Rodrigues, R.; Pereira, E. Fingerprinting an oil spill event (August of 2021) in the oceanic Fernando de Noronha archipelago using biomarkers and stable carbon isotopes. *Mar. Pollut. Bull.* **2022**, *185*, No. 114316.

(8) Pereira, M. G.; Santos, I. R.; Lima, I. F.; Coutinho, M. E. B.; Carregosa, J. C.; Wisniewski, A.; Santos, J. M. Geochemical Assessment of Tar Balls That Arrived in 2022 along the Northeast Coast of Brazil and Their Relationship with the 2019 Oil Spill Disaster. *Energy Fuels* **2023**, *37*, 16388−16395.

(9) Corrêa, A. M.; Campos, F. F.; Tenório, M. F.; Rodrigues, A. M. S.; Pérez, C. D.; Thompson, F.; Batista, A. S.; Gatts, P. V.; de Rezende, C. E.; Leal, K. Z.; Bernardes, M. C. Hydrocarbon composition of oils spilt on the Brazilian coast in 2019 and 2022. *Mar. Pollut. Bull.* **2024**, *207*, No. 116821.

(10) Martins, L. L.; Pereira, V. B.; Nascimento, A. P.; Azevedo, R. N. A.; Oliveira, A. H.; Teixeira, C. E. P.; Azevedo, D. A.; da Cruz, G. F.; Cavalcante, R. M.; Giarrizzo, T. Forensic Geochemistry Reveals International Ship Dumping as a Source of New Oil Spill in Brazil's Coastline (Bahia) in Late 2023. *Environ. Sci. Technol.* **2024**, *58*, 9328−9338.

(11) Nascimento, A. P.; Azevedo, R. N. A.; Pereira, M. G. A.; Franco, D. M. M.; Vaz, B. G.; Oliveira, A. H. B.; Santos, J. M.; Cavalcante, R. M.; Martins, L. L. Forensic environmental geochemistry to reveal the extent, characteristics, and fate of waxy tarballs spilled over the northeast coast of Brazil in 2022. *Mar. Environ. Res.* **2025**, No. 106878.

(12) Soares, M. O.; Rabelo, E. F.; Mathews-Cascon, H. Intertidal anthozoans from the coast of Ceará. *Rev. Bras. Biocîenc.* **2011**, *9*, 437.

(13) Soares, M. D. O.; Rossi, S.; Martins, F. A. S.; Carneiro, P. B. D. M. The forgotten reefs: benthic assemblage coverage on a sandstone reef (Tropical South-western Atlantic). *J. Mar. Biol. Assoc. U. K.* **2017**, *97*, 1585−1592.

(14) Costa, A. C. P.; Garcia, T. M.; Paiva, B. P.; Ximenes Neto, A. R.; Soares, M. d. O. Seagrass and rhodolith beds are important seascapes for the development of fish eggs and larvae in tropical coastal areas. *Mar. Environ. Res.* **2020**, *161*, No. 105064.

(15) Carneiro, P. B. d. M.; Lima, J. P. d.; Bandeira, Ê. V. P.; Ximenes Neto, A. R.; Rocha Barreira, C. d. A.; Tâmega, F. T. d. S.; Matthews-Cascon, H.; Franklin Junior, W.; Morais, J. O. d. Structure, growth and $CaCO_3$ production in a shallow rhodolith bed from a highly energetic siliciclastic-carbonate coast in the equatorial SW Atlantic Ocean Rhodolith bed structure and production under energetic conditions. *Mar. Environ. Res.* **2021**, *166*, No. 105280.
(16) Carneiro, P. B. M.; Ximenes Neto, A. R.; Jucá-Queiroz, B.; Teixeira, C. E. P.; Feitosa, C. V.; Barroso, C. X.; Matthews-Cascon, H.; de Morais, J. O.; Freitas, J. E. P.; Santander-Neto, J.; de Araújo, J. T.; Monteiro, L. H. U.; Pinheiro, L. S.; Braga, M. D. A.; Cordeiro, R. T. S.; Rossi, S.; Bejarano, S.; Salani, S.; Garcia, T. M.; Lotufo, T. M. C.; Smith, T. B.; Faria, V. V.; Soares, M. O. Interconnected marine habitats form a single continental-scale reef system in South America. *Sci. Rep.* **2022**, *12*, 17359.
(17) Soares, M. O.; Brandão, D. B.; Teixeira, C. E. P.; Cavalcante, R. M.; Oliveira, A. H. B. d.; Bezerra, L. E. A.; Barros, E. L. Déjà vu: New oil spill poses cumulative risks to protected coastal environments in the South Atlantic. *Mar. Policy* **2023**, *155*, No. 105764.
(18) Bérgamo, D. B.; Craveiro, N.; Magalhães, K. M.; Yogui, G. T.; Soares, M. O.; Zanardi-Lamardo, E.; Rojas, L. A. V.; Lima, M. C. S. d.; Rosa Filho, J. S. Tar balls as a floating substrate for long-distance species dispersal. *Mar. Pollut. Bull.* **2023**, *196*, No. 115654.
(19) Dong, Y.; Liu, Y.; Hu, C.; MacDonald, I. R.; Lu, Y. Chronic oiling in global oceans. *Science.* **2022**, *376*, 1300−1304.
(20) Kvenvolden, K. A.; Cooper, C. K. Natural seepage of crude oil into the marine environment. *Geo-Mar. Lett.* **2003**, *23*, 140−146.
(21) Burgherr, P. In-depth analysis of accidental oil spills from tankers in the context of global spill trends from all sources. *J. Hazard. Mater.* **2007**, *140*, 245−256.
(22) Chen, J.; Zhang, W.; Wan, Z.; Li, S.; Huang, T.; Fei, Y. Oil spills from global tankers: Status review and future governance. *J. Clean. Prod.* **2019**, *227*, 20−32.
(23) Scarlett, A. G.; Nelson, R. K.; Gagnon, M. M.; Holman, A. I.; Reddy, C. M.; Sutton, P. A.; Grice, K. MV Wakashio grounding incident in Mauritius 2020: The world's first major spillage of Very Low Sulfur Fuel Oil. *Mar. Pollut. Bull.* **2021**, *171*, No. 112917.
(24) Speight, J. G.*Handbook of petroleum product analysis*. John Wiley & Sons. 2015.
(25) Uhler, A. D.; Stout, S. A.; Douglas, G. S.; Healey, E. M.; Emsbo-Mattingly, S. D.Chemical character of marine heavy fuel oils and lubricants. In *Standard Handbook Oil Spill Environmental Forensics*; Academic Press. 2016; pp 641−683. .
(26) Wang, Z.; Yang, C.; Yang, Z.; Brown, C. E.; Hollebone, B. P.; Stout, S. A. Petroleum biomarker fingerprinting for oil spill characterization and source identification. In *Standard Handbook Oil Spill Environmental Forensics*; Academic Press, 2016; pp 131−254. .
(27) Nelson, R. K.; Scarlett, A. G.; Gagnon, M. M.; Holman, A. I.; Reddy, C. M.; Sutton, P. A.; Grice, K. Characterizations and comparison of low sulfur fuel oils compliant with 2020 global sulfur cap regulation for international shipping. *Mar. Pollut. Bull.* **2022**, *180*, No. 113791.
(28) Scarlett, A. G.; Nelson, R. K.; Gagnon, M. M.; Reddy, C. M.; Grice, K. MV Very low sulfur fuel oil spilled from the MV Wakashio in 2020 remains in sediments in a Mauritius mangrove ecosystem nearly three years after the grounding. *Mar. Pollut. Bull.* **2024**, *209*, No. 117283.
(29) Osipova, L.; Georgeff, E.; Comer, B. Global scrubber washwater discharges under IMO's 2020 fuel sulfur limit. *Int. Counc. Clean Transp.* **2021**, 10−12.
(30) Gondikas, A.; Mattsson, K.; Hassellöv, M. A new form of hazardous microparticulate contamination to the marine environment from ships using heavy fuel oil with exhaust gas scrubbers−Characterization and implications for fate, transport and ecotoxicity. *Sci. Total Environ.* **2025**, *959*, No. 178263.
(31) Brown, K.; Ptácek, S.; Gamble, J.; Carr, E.; McCabe, S. Poison in the water: the call to ban scrubber discharge, The health and environmental costs industry wants us to ignore. *Pacific Environment* **2025**, 1−47. https://www.pacificenvironment.org/wp-content/uploads/2025/01/Poison-in-the-water.pdf
(32) *Changzhou Fengdi Plastic Technology*. 2024, https://www.cube-bag.com/sdp/2391156/4/cp-7738910/0/Sample_Bottles_Spares.html (assessed September 1, 2024).
(33) *Standard Club Part of Northstandard*. 2019, https://www.standard-club.com/knowledge-news/article-sampling-of-fuel-oil-used-on-board-psc-enforcement-criteria-1114/ (assessed March 15, 2025).
(34) *International Maritime Organization*. 2024, https://www.imo.org/en/ourwork/environment/pages/index-of-mepc-resolutions-and-guidelines-related-to-marpol-annex-vi.aspx (assessed March 15, 2025).
(35) Lima, B. D.; Martins, L. L.; Pereira, V. B.; Franco, D. M.; Dos Santos, I. R.; Santos, J. M.; Vaz, B. G.; Azevedo, D. A.; da Cruz, G. F. Weathering impacts on petroleum biomarker, aromatic, and polar compounds in the spilled oil at the northeast coast of Brazil over time. *Mar. Pollut. Bull.* **2023**, *189*, No. 114744.
(36) Demirbas, A.; Taylan, O. Removing of resins from crude oils. *Pet. Sci. Technol.* **2016**, *34*, 771−777.
(37) Kieu, H. T.; Law, A. W. K. Determination of surface film thickness of heavy fuel oil using hyperspectral imaging and deep neural networks. *Int. J. Remote Sens.* **2022**, *43*, 997−1014.
(38) Aljaziri, J.; Gautam, R.; Sarathy, S. M. Interactions in co-pyrolysis of Salicornia bigelovii and heavy fuel oil. *Sustain. Energy Fuels* **2023**, *7*, 4213−4228.
(39) Fingas, M.*Handbook of oil spill science and technology*. John Wiley & Sons, 2014.
(40) Douglas, G. S.; Stout, S. A.; Uhler, A. D.; McCarthy, K. J.; Emsbo-Mattingly, S. D.Advantages of quantitative chemical fingerprinting in oil spill identification and allocation of mixed hydrocarbon contaminants. In *Standard Handbook Oil Spill Environmental Forensics*; Academic Press. 2016; pp 789−847. .
(41) Yang, C.; Wang, Z.; Yang, Z.; Hollebone, B.; Fieldhouse, B.; Lambert, P.; Fingas, M. Chemical fingerprints and chromatographic analysis of crude oils and petroleum products. *Chemistry of Oil and Petroleum Products* **2022**, 47.
(42) López, L.; Lo Mónaco, S.; Richardson, M. Use of molecular parameters and trace elements in oil-oil correlation studies, Barinas sub-basin. *Venezuela. Org. Geochem.* **1998**, *29*, 613−629.
(43) Peters, K. E.; Moldowan, J. M. The Biomarker Guide. Interpreting Molecular Fossils in Petroleum and Ancient Sediments. *Prentice Hall, New Jersey* **1993**, 363.
(44) Liu, X.; Wang, Z.; Ma, X.; Xu, H.; Yao, Z. Distinguishing crude oils from heavy fuel oils by polycyclic aromatic hydrocarbon fingerprints. *Environ. Forensics.* **2013**, *14*, 20−24.
(45) Zhang, H.; Wang, C.; Zhao, R.; Yin, X.; Zhou, H.; Tan, L.; Wang, J. New diagnostic ratios based on phenanthrenes and anthracenes for effective distinguishing heavy fuel oils from crude oils. *Mar. Pollut. Bull.* **2016**, *106*, 58−61.
(46) Emsbo-Mattingly, Stephen D.; Eric, Litman Polycyclic aromatic hydrocarbon homolog and isomer fingerprinting. In *Standard Handbook Oil Spill Environmental Forensics*; Academic Press. 2016; pp 255−312. .
(47) Stout, S. A.; Douglas, G. S.; Uhler, A. D.Chemical fingerprinting of gasoline and distillate fuels. In *Standard Handbook Oil Spill Environmental Forensics*; Academic Press. 2016; pp 509−564. http://dx.doi.org/.
(48) Wang, Z.; Fingas, M. Use of methyldibenzothiophenes as markers for differentiation and source identification of crude and weathered oils. *Environ. Sci. Technol.* **1995**, *29*, 2842−2849.
(49) Wang, Z.; Fingas, M.; Page, D. S. Oil spill identification. *J. Chromatogr. A* **1999**, *843*, 369−411.
(50) Schueppel, M.; Graebner, M. Pyrolysis of Heavy Fuel Oil (HFO)−A review on physicochemical properties and pyrolytic decomposition characteristics for application in novel, industrial-scale HFO pyrolysis technology. *J. Anal. Appl. Pyrolysis* **2024**, *179*, No. 106432.
(51) Hwang, H. M.; Stanton, B.; McBride, T.; Anderson, M. J. Polycyclic aromatic hydrocarbon body residues and lysosomalmembrane destabilization in mussels exposed to the Dubai Starbunker fuel

oil (intermediate fuel oil 380) spill in San Francisco Bay. *Environ. Toxicol. Chem.* **2014**, *33*, 1117−1121.
(52) Speight, J. G.*Shale oil and gas production processes*. Gulf Professional Publishing. 2019.
(53) Mirshafiee, F.; Movahedirad, S.; Sobati, M. A.; Alaee, R.; Zarei, S.; Sargazi, H. Current status and future prospects of oxidative desulfurization of naphtha: a review. *Process Saf. Environ. Prot.* **2023**, *170*, 54−75.
(54) Tian, Y.; Jiang, B.; Chen, J.; Zhan, Z. W.; Yang, C.; Zou, Y. R.; Peng, P. Characterisation by ESI FT-ICR MS of heteroatomic compounds in catalytic hydropyrolysates released from marine crude oil asphaltenes. *Org. Geochem.* **2022**, *167*, No. 104391.
(55) Dalmaschio, G. P.; Malacarne, M. M.; de Almeida, V. M.; Pereira, T. M.; Gomes, A. O.; de Castro, E. V.; Greco, S. J.; Vaz, B. G.; Romão, W. Characterization of polar compounds in a true boiling point distillation system using electrospray ionization FT-ICR mass spectrometry. *Fuel.* **2014**, *115*, 190−202.
(56) Stanford, L. A.; Kim, S.; Rodgers, R. P.; Marshall, A. G. Characterization of compositional changes in vacuum gas oil distillation cuts by electrospray ionization fourier transform− ion cyclotron resonance (FT− ICR) mass spectrometry. *Energy Fuels* **2006**, *20*, 1664−1673.
(57) Smith, D. F.; Rahimi, P.; Teclemariam, A.; Rodgers, R. P.; Marshall, A. G. Characterization of Athabasca bitumen heavy vacuum gas oil distillation cuts by negative/positive electrospray ionization and automated liquid injection field desorption ionization Fourier transform ion cyclotron resonance mass spectrometry. *Energy Fuels* **2008**, *22*, 3118−3125.
(58) Faksness, L. G.; Leirvik, F.; Taban, I. C.; Engen, F.; Jensen, H. V.; Holbu, J. W.; Dolva, H.; Bråtveit, M. Offshore field experiments with in-situ burning of oil: Emissions and burn efficiency. *Environ. Res.* **2022**, *205*, No. 112419.
(59) Reddy, C. M.; Arey, J. S.; Seewald, J. S.; Sylva, S. P.; Lemkau, K. L.; Nelson, R. K.; Carmichael, C. A.; McIntyre, C. P.; Fenwick, J.; Ventura, G. T.; Mooy, B. A. S. V.; Camilli, R. Composition and fate of gas and oil released to the water column during the Deepwater Horizon oil spill. *Proc. Natl. Acad. Sci. U. S. A.* **2012**, *109*, 20229−20234.
(60) Chen, H.; Nelson, R. K.; Swarthout, R. F.; Shigenaka, G.; de Oliveira, A. H.; Reddy, C. M.; McKenna, A. M. Detailed compositional characterization of the 2014 Bangladesh furnace oil released into the world's largest mangrove forest. *Energy Fuels.* **2018**, *32*, 3232−3242.
(61) Lemkau, K. L.; McKenna, A. M.; Podgorski, D. C.; Rodgers, R. P.; Reddy, C. M. Molecular evidence of heavy-oil weathering following the M/V Cosco Busan spill: insights from Fourier transform ion cyclotron resonance mass spectrometry. *Environ. Sci. Technol.* **2014**, *48*, 3760−3767.
(62) Swarthout, R. F.; Nelson, R. K.; Reddy, C. M.; Hall, C. G.; Boufadel, M.; Valentine, D.; Arey, J. S.; Gros, J. *Physical and Chemical Characterization of Canadian Dilbit and Related Products* 2015.
(63) Sørensen, M. K.; Vinding, M. S.; Bakharev, O. N.; Nesgaard, T.; Jensen, O.; Nielsen, N. C. NMR sensor for onboard ship detection of catalytic fines in marine fuel oils. *Anal. Chem.* **2014**, *86*, 7205−7208.
(64) Atkinson, D. Determining Catalytic Fines Concentrations in Heavy Fuel Oils. *MTZ. Ind.* **2017**, *7*, 50−57.
(65) Vedachalam, S.; Baquerizo, N.; Dalai, A. K. Review on impacts of low sulfur regulations on marine fuels and compliance options. *Fuel* **2022**, *310*, No. 122243.
(66) Krewski, D.; Yokel, R. A.; Nieboer, E.; Borchelt, D.; Cohen, J.; Harry, J.; Kacew, S.; Lindsay, J.; Mahfouz, A. M.; Rondeau, V. Human health risk assessment for aluminium, aluminium oxide, and aluminium hydroxide. *J. Toxicol. Environ. Health B Crit. Rev.* **2007**, *10*, 1−269.
(67) Esfandyari Bayat, A.; Junin, R.; Shamshirband, S.; Tong Chong, W. Transport and retention of engineered Al_2O_3, TiO_2 and SiO_2 nanoparticles through various sedimentary rocks. *Sci. Rep.* **2015**, *5*, 14264.
(68) Bryliński, Ł.; Kostelecka, K.; Woliński, F.; Duda, P.; Góra, J.; Granat, M.; Flieger, J.; Teresiński, G.; Buszewicz, G.; Sitarz, R.; Baj, J. Aluminium in the human brain: routes of penetration, toxicity, and resulting complications. *Int. J. Mol. Sci.* **2023**, *24*, 7228.
(69) Magalhães, K. M.; Rosa Filho, J. S.; Teixeira, C. E. P.; Coelho, C., Jr.; Lima, M. C. S.; Costa Souza, A. M.; Soares, M. O. Oil and plastic spill: 2021 as another challenging year for marine conservation in the South Atlantic Ocean. *Marine Policy.* **2022**, *140*, No. 105076.
(70) Carmichael, C. A.; Arey, J. S.; Graham, W. M.; Linn, L. J.; Lemkau, K. L.; Nelson, R. K.; Reddy, C. M. Floating oil-covered debris from Deepwater Horizon: identification and application. *Environ. Res. Lett.* **2012**, *7*, No. 015301.
(71) Stout, S. A.; Wang, Z.Chemical fingerprinting methods and factors affecting petroleum fingerprints in the environment. In *Standard Handbook Oil Spill Environmental Forensics*; Academic Press, 2016; pp 61−129. ..
(72) Peters, K. E.; Walters, C. C.; Moldowan, J. M.*The Biomarker Guide: Biomarkers and Isotopes in the Petroleum Exploration and Earth History*, 2nd ed., University Press: Cambridge, Vol. 2. 2005.
(73) Tissot, B. P.; Welte, D. H.*Petroleum Formation and Occurrence*. Springer-Verlag: New York. 1984.
(74) Mello, M. R.; Telnaes, N.; Maxwell, J. R.The hydrocarbon source potential in the Brazilian marginal basins: a geochemical and paleoenvironmental assessment. In: *Paleogeography, Paleoclimate, and Source Rocks* (A.-Y., Huc, ed.), American Association of Petroleum Geologists: Tulsa, OK. 1995; pp 233−72.
(75) Holba, A. G.; Dzou, L. I.; Wood, G. D.; Ellis, L.; Adam, P.; Schaeffer, P.; Albrecht, P.; Greene, T.; Hughes, W. B. Application of tetracyclic polyprenoids as indicators of input from fresh-brackish water environments. *Org. Geochem.* **2003**, *34*, 441−469.
(76) Mackenzie, A. S.; Patience, R. L.; Maxwell, J. R.; Vandenbroucke, M.; Durand, B. Molecular parameters of maturation in the Toarcian shales, Paris Basin, France − I. Changes in the configuration of acyclic isoprenoid alkanes, steranes, and triterpanes. *Geochim. Cosmochim. Acta* **1980**, *44*, 1709−21.
(77) Seifert, W. K.; Moldowan, J. M; Jones, R. W.Application of biological marker chemistry to petroleum exploration. In: *Proceedings of the Tenth World Petroleum Congress*; Heyden & Son, Inc.: Philadelphia. 1980, PA pp 425−40.
(78) Arekhi, M.; Terry, L. G.; John, G. F.; Clement, T. P. Environmental fate of petroleum biomarkers in Deepwater Horizon oil spill residues over the past 10 years. *Sci. Total Environ.* **2021**, *791*, No. 148056.
(79) Reddy, C. M.; Quinn, J. G. GC-MS analysis of total petroleum hydrocarbons and polycyclic aromatic hydrocarbons in seawater samples after the North Cape oil spill. *Mar. Pollut. Bull.* **1999**, *38*, 126−135.
(80) Lemkau, K. L.; Peacock, E. E.; Nelson, R. K.; Ventura, G. T.; Kovecses, J. L.; Reddy, C. M. The M/V Cosco Busan spill: Source identification and short-term fate. *Mar. Pollut. Bull.* **2010**, *60*, 2123−2129.
(81) Ryan, P. G.; Dilley, B. J.; Ronconi, R. A.; Connan, M. Rapid increase in Asian bottles in the South Atlantic Ocean indicates major debris inputs from ships. *Proceedings of the National Academy of Sciences.* **2019**, *116*, 20892−20897.
(82) Ryan, P. G.; Weideman, E. A.; Perold, V.; Hofmeyr, G.; Connan, M. Message in a bottle: Assessing the sources and origins of beach litter to tackle marine pollution. *Environ. Pollut.* **2021**, *288*, No. 117729.

https://doi.org/10.1021/acs.energyfuels.5c01581
Energy Fuels 2025, 39, 14254−14265